

LG Semicon Company, Limited, assisted in meeting the publication costs of this article.

REFERENCES

- J. Bevk, M. Furttsch, G. E. Georgiou, S. J. Hillenius, D. Schielein, T. Schiml, P. J. Silverman, and H. S. Luftman, *Mater. Res. Soc. Symp. Proc.*, **429**, 115 (1996).
- K. C. Saraswat, D. L. Brors, J. A. Fair, K. A. Monning, and R. Beyers, *IEEE Trans. Electron Devices*, **ED-30**, 1497 (1983).
- Y. Shioya and M. Maeda, *J. Appl. Phys.*, **60**, 327 (1986).
- Y. Shioya, S. Kawamura, I. Kobayashi, M. Maeda, and K. Yanagida, *J. Appl. Phys.*, **61**, 5102 (1987).
- G. Giroult, A. Nouailhat, M. Gauneau, *J. Appl. Phys.*, **67**, 515 (1990).
- C. S. Yoo, T. H. Lin, N. S. Tsai, and L. J. Ijzendoorn, *Jpn. J. Appl. Phys.*, **29**, 2535 (1990).
- T. Hara, T. Miyamoto, and T. Yokoyama, *J. Electrochem. Soc.*, **136**, 1177 (1989).
- T. Hara, T. Miyamoto, H. Hagiwara, E. I. Bromley, and W. R. Harshbarger, *J. Electrochem. Soc.*, **137**, 2955 (1990).
- J. T. Hillman, W. M. Triggs, and M. Aruga, *J. Electrochem. Soc.*, **139**, 3574 (1992).
- S. G. Telford, M. Eizenberg, M. Chang, A. K. Sinha, and T. R. Gow, *J. Electrochem. Soc.*, **140**, 3689 (1993).
- S. G. Telford, M. Eizenberg, M. Chang, A. K. Sinha, and T. R. Gow, *Appl. Phys. Lett.*, **62**, 1766 (1993).
- Y. W. Kim, N. I. Lee, and M. H. Park, *Mater. Res. Soc. Symp. Proc.*, **355**, 491 (1995).
- Y. Akasaka, S. Suehiro, K. Nakajima, T. Nakasugi, K. Miyano, K. Kasai, H. Oyamatsu, M. Kinugawa, M. T. Takaki, K. Agawa, F. Matsuoka, M. Kakumu, and K. Suguro, *IEEE Trans. Electron Devices*, **ED-43**, 1864 (1996).
- M. T. Takaki, K. Miyashita, H. Koyama, K. Nakajima, K. Miyano, Y. Akasaka, Y. Hiura, S. Inaba, A. Azuma, H. Koike, H. Yoshimura, K. Suguro, and H. Ishiuchi, *Tech. Dig. Int. Electron Devices Meet.*, 455 (1996).
- H. Wakabayashi, T. Andoh, K. Sato, K. Yoshida, H. Miyamoto, T. Mogami, and T. Kunio, *Tech. Dig. Int. Electron Devices Meet.*, 447 (1996).
- D. L. Bae, E. H. Lee, H. S. Kim, G. H. Choi, D. H. Ko, H. K. Kang, and M. Y. Lee, in *Proceedings of VMIC Conference*, pp. 521-523 (1996).
- J. S. Byun, B. H. Lee, J. S. Park, and J. J. Kim, *J. Electrochem. Soc.*, **144**, 3572 (1997).
- JCPDS Card No. 11-0915, International Center for Diffraction Data, Swarthmore, PA.
- F. M. d'Heurle, C. S. Peterson, and M. Y. Tsai, *J. Appl. Phys.*, **51**, 5796 (1980).
- R. Palmans, B. Vermeire, and K. Maex, *Mater. Res. Soc. Symp. Proc.*, **ULSI IX**, 489 (1994).
- C. L. Huang and N. D. Arora, *IEEE Trans. Electron Devices*, **ED-40**, 2330 (1993).
- R. Rios, N. D. Arora, C. L. and Huang, *IEEE Electron Device Lett.*, **EDL-15**, 129 (1994).
- T. Hosoya, K. Machida, K. Imai, and E. Arai, *IEEE Trans. Electron Devices*, **ED-42**, 2111 (1993).

Influence of Deposition Parameters on the Texture of Chemical Vapor Deposited Tungsten Films by a $WF_6/H_2/Ar$ Gas Source

I-Shun Chang and Min-Hsiung Hon

Department of Materials Science and Engineering, National Cheng Kung University, Tainan, Taiwan

ABSTRACT

In order to investigate the relationship between the film texture and the deposition parameters including gas composition, temperatures, and substrate materials, polycrystalline tungsten films were prepared by reduction of tungsten hexafluoride with hydrogen. The experimental results show that the orientations of the textured films correlate closely with WF_6 concentrations in the gas mixture and deposition temperatures. High WF_6 concentrations enhance the formation of the $\langle 100 \rangle$ textured films, while low WF_6 concentrations facilitate the formation of the $\langle 111 \rangle$ textured films. The $\langle 111 \rangle$ texture, usually observed in tungsten films deposited at high temperatures ($\geq 400^\circ C$) and high ratios of H_2 to WF_6 , can also form at low deposition temperatures ($370^\circ C$) when the WF_6 concentration used is low enough (0.6 vol %). The WF_6 concentration for obtaining a $\langle 100 \rangle$ textured film increases with increasing deposition temperatures. On the other hand, the concentrations of hydrogen gas have minimal influence on the formation of the film textures. Therefore, in terms of gas composition, the WF_6 concentration, not the ratio of H_2 to WF_6 , is a compact factor which directly dominates the texture of the films. The effect of substrate on the film texture was only found in the initial growth stage. The crystals formed at the beginning of the film growth were randomly oriented. A preferential orientation became pronounced with increasing film thickness through the competitive crystal growth.

Introduction

Crystallographic texture is commonly observed in films prepared by vapor deposition techniques. For tungsten films deposited by chemical vapor deposition (CVD) process using tungsten hexafluoride (WF_6) and hydrogen (H_2) as precursors, either the $\langle 100 \rangle$ or $\langle 111 \rangle$ texture is frequently observed depending on the deposition conditions.¹⁻⁵ McMurray et al.¹ concluded that the $\langle 100 \rangle$ growth is favored by the conditions of low ratios of hydrogen to tungsten hexafluoride gas mixture and substrate temperatures, while high H_2 ratios (≥ 60) and substrate temperatures ($\geq 600^\circ C$) favor the $\langle 111 \rangle$ growth. Schroff et al.² mentioned that under the conditions of very rich hydrogen content atmosphere, the $\langle 111 \rangle$ textured tungsten films could be obtained. However, the $\langle 111 \rangle$ texture was observed for films deposited with the H_2/WF_6 ratio of 27 at temperature of $400^\circ C$.³ Chuzhko et al.⁴ found that the preferred orientation of tungsten films changes along the deposition tube, from

the $\langle 100 \rangle$ orientation for films formed at the inlet of the tube to the $\langle 111 \rangle$ orientation for films formed close to the outlet of the tube, and explained that a higher concentration of tungsten hexafluoride in atmosphere is necessary for the growth of the $\langle 100 \rangle$ textured films. Obviously, a detailed study of texture growth as a function of the individual deposition parameters is still not available.

The objective of this work was to investigate the relationship among variation of orientations, composition of gas mixtures, and deposition temperatures. In addition, the effect of substrate on the formation of film texture was also evaluated, and the experimental results were discussed.

Experimental

A conventional hot wall CVD system, as shown in Fig. 1, with H_2-WF_6-Ar gas mixtures was utilized to prepare the tungsten films. The inner diameter of the chamber was 40 mm. The temperature in the isothermal zone was $610 \pm 2^\circ C$ for 7 cm. The reactants were delivered into the reaction

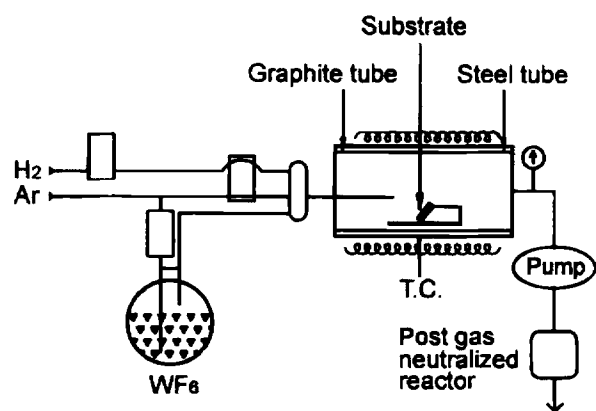


Fig. 1. Schematic diagram of CVD apparatus used in the experiment.

zone by a water-cooled pipe to attenuate the preconsumption on the delivery path. The amount of tungsten hexafluoride added was controlled by the flow of argon carrier gas through a bottle containing liquid WF_6 and by the temperature of the bottle. The tube was evacuated and purged with hydrogen during heating to insure cleanliness. To investigate the change of preferred orientation in tungsten deposit, 200–1600 standard cubic centimeters per minute (sccm) of hydrogen (12–94 vol %) and 10–80 sccm of WF_6 (0.6–4.7 vol %) were selected to keep the ratios of H_2/WF_6 selected covering a wide range from sub- to superstoichiometry of the reaction: $WF_6 + 3H_2 \rightleftharpoons W + 6HF$. The deposition temperatures of 610 and 490°C were used because it was found from the previous experiments that the change of texture from $\langle 100 \rangle$ to $\langle 111 \rangle$ appears at temperatures $\geq 550^\circ C$ for most deposition conditions in this work. The pressure in the chamber during deposition was set at 200 Torr and the total gas flow rate was kept constantly at 1700 sccm by Ar gas supplement.

Graphite plates with a dimension of $10 \times 20 \times 2$ mm were used as substrates. When the effect of substrate on the formation of film texture was studied, the underlayer of either the $\langle 100 \rangle$ or $\langle 111 \rangle$ textured tungsten films were first deposited before the normal deposition. In addition, the n-type Si(111) wafers and metal Ni plates were also used. For the substrate preparation, the graphite plates were ground by no. 1200 abrasive paper, and the Ni plates were polished by 1 μm alumina powder, respectively. To determine the dependence of the film texture on the film thickness, films with various thicknesses were prepared at different deposition conditions. On the other hand, a 30 μm thick $\langle 100 \rangle$ textured tungsten sample was thinned

successively by grinding, and the X-ray diffraction (XRD) analyses were conducted for different film thicknesses.

The film textures were evaluated with the texture coefficient (TC) values determined by XRD spectra (Cu $K\alpha$ radiation, scanning range from 39 to 118 for 2θ degrees). TC values were expressed as follows⁶

$$TC_{\{hkl\}} = \frac{I_{\{hkl\}}^m}{\frac{1}{n} \sum_1^n \left(\frac{I_{\{hkl\}}^m}{I_{\{hkl\}}^o} \right)}$$

where $TC_{\{hkl\}}$ is the texture coefficient for a specific lattice plane $\{hkl\}$ in the measured films, n is the total number of diffraction peaks calculated, and $I_{\{hkl\}}^m$ and $I_{\{hkl\}}^o$ are the relative intensity of the $\{hkl\}$ peak for a measured film and for a randomly oriented sample, respectively. The JCPDS (Joint Committee on Powder Diffraction Standards)⁷ value, however, was used as $I_{\{hkl\}}^o$ in the present study. For each sample, the five $\{hkl\}$ peaks with large ratio of ($I_{\{hkl\}}^m/I_{\{hkl\}}^o$) were used to calculate their corresponding TC values. In most cases, they were $\{110\}$, $\{200\}$, $\{211\}$, $\{310\}$, and $\{222\}$. If the $TC_{\{hkl\}}$ value is greater than 1, the film has an $\langle hkl \rangle$ preferred orientation. The greater the TC value, the higher degree is the preferred orientation. Most of the film depositions were conducted twice, and the results are reproducible.

Results and Discussion

The change on TC values accompanying the change on WF_6 concentrations were examined on films deposited under various deposition conditions: poor (samples 1–3 and 7–9) and rich (samples 4–6 and 10–13) H_2 atmospheres at temperatures of 610°C (samples 1–6) and 490°C (samples 7–13), as shown in Table I. Increased WF_6 concentrations tend to form the $\langle 100 \rangle$ textured films rather than the $\langle 111 \rangle$ ones; the latter were obtained at low WF_6 concentrations. For example, the films deposited at a WF_6 concentration of 0.6 vol %, over the temperatures described here, all show the $\{111\}$ plane with the largest TC value (except sample 10 which is thinner and has a more random distribution of orientations), i.e., these films exhibit a $\langle 111 \rangle$ preferred orientation. As the WF_6 concentration increases to 2.4 or 4.8 vol %, the texture coefficient of $\{200\}$ plane ($TC_{\{200\}}$) becomes the largest one whereas $TC_{\{222\}}$ decreases drastically; hence, the $\langle 100 \rangle$ texture forms in the tungsten films. The required WF_6 concentrations for the texture transition from the $\langle 111 \rangle$ to $\langle 100 \rangle$ depends on deposition temperatures. For example, 4.8 vol % WF_6 is needed at 610°C, while only 2.4 vol % is required at 490°C. The films were $\langle 310 \rangle$ textured when deposited under a narrow range of conditions, e.g., a low H_2 concentration (12 vol %) coupled with low ratios of H_2/WF_6 (close

Table I. Texture coefficients of CVD tungsten films as a function of WF_6 concentrations. [Deposition pressure = 200 Torr, total flow = 1700 sccm, Ar gas = balanced, and substrate = graphite.]

Sample no.	Precursors (vol %)		Film deposition temp (°C)	Thickness (μm)	Texture coefficients				
	H_2	WF_6			$\{110\}$	$\{200\}$	$\{211\}$	$\{310\}$	$\{222\}$
1	12	0.6	610	8.6	0.3	0.5	1.2	0.2	2.8
2	12	2.4	610	15	0.3	1.1	0.4	3.1	— ^a
3	12	4.7	610	29	0.1	0.3	0.3	4.3	—
4	47	0.6	610	14	0.0	0.0	—	—	5.0
5	47	2.4	610	38	0.0	0.0	0.1	—	4.9
6	47	4.7	610	40	0.0	2.4	0.6	0.2	1.8
7	12	0.6	490	9	0.8	0.5	1.4	0.9	1.4
8	12	2.4	490	9.5	0.2	1.7	0.9	1.6	0.6
9	12	4.7	490	6.6	0.5	2.2	0.6	1.3	0.4
10	47	0.6	490	2.0	1.1	0.7	1.4	0.8	1.0
11	47	0.6	490	17	0.2	0.1	0.5	0.1	4.1
12	47	2.4	490	31	0.0	5.0	—	—	—
13	47	4.7	490	17	0.1	4.3	0.1	0.4	—

^a The mark “—” means the corresponding diffraction peak was not found in the spectrum, while the peak with calculated value of 0.0 is of very small relative intensity.

to five or less) and high substrate temperature (610°C), as represented by samples 2 and 3.

Table II shows the dependence of crystallographic texture on H₂ concentrations for films deposited at various WF₆ concentrations and deposition temperatures (samples above the dotted line). Increasing the H₂ concentration from 12 to 94 vol % does not alter the largest TC value- lattice plane (except sample 2), which was determined primarily by both WF₆ concentrations and deposition temperatures. For example, {222} plane is the one with the largest TC value for each sample in the two series of samples 1, 4, 15 and samples 7, 11, 16, while TC_{200} is the largest for samples 8, 12 and 18. In other words, the film texture is insensitive to the change of H₂ concentrations during deposition. Based on the results, it can be known that if the ratio of H₂ to WF₆ concentration remains unchanged, the increase of reactant concentration in gas atmosphere will favor the formation of the <100> textured films more than that of the <111> ones. It has been illustrated by the sets of samples 7, 12, 21, and samples 1, 5, 19, showing the <111> texture at low reactant concentrations and, however, the <100> at medium or high reactant concentrations.

The effect of H₂ on the film texture observed here is not consistent with that proposed by Schroff et al.² and Blocher,⁸ who mentioned that a high H₂ content in gas phase would lead to a <111> oriented film. Since the experimental details were not given in the papers, further discussion about the difference between the present results and theirs is not allowed to proceed. McMurry et al.¹ reported that the most significant factor determining the film texture is the hydrogen-tungsten hexafluoride ratio, a large value of which leads to a <111> textured film, while a low value leads to a <100> textured film. Nevertheless, their results showed a fact that a <100> textured film can be formed when a large enough amount of WF₆ was used even at the conditions of the largest H₂/WF₆ ratio of 60 in Table II.¹ Taking this into account, the H₂ to WF₆ ratio seems not to be the only significant orientation-controlling factor as the authors concluded. The WF₆ concentration is also an important term which affects readily the evolution of orientations in tungsten films.

The film texture is also affected by deposition temperatures. The texture changed from the <100> to a <111> orientation with increasing deposition temperature from 490 to 610°C, as revealed by comparing sample 5 with 12 (or 17 with 18) in Table II. High deposition temperature, however, favors the formation of the <111> textured films, but it is not indispensable to the <111> texture growth. With a

low enough WF₆ concentration, for example, 0.6 vol % in the present experiments, a <111> textured film can be deposited at a substrate temperature as low as 370°C.

It follows that the crystallographic texture of tungsten film depends strongly on WF₆ concentrations and deposition temperatures but weakly on H₂ concentrations. The film is <100> textured when the WF₆ concentration used is larger than some value which increases with increasing deposition temperatures. For example, the value was larger than 0.6 and 2.4 vol % for a <100> textured film deposited at 490 and 610°C, respectively. On the opposite side, the films were <111> textured when deposited with a low WF₆ concentration of 0.6 vol % over the entire range of deposition temperatures (370-610°C). The film texture was found insensitive to the H₂ concentration when the value of H₂/WF₆ ratio is greater than about 5. It was also observed that the factors dictating the film texture are not the same as those dictating the growth rate which strongly depend on H₂ concentrations (of 1/2 order) and deposition temperatures (with activation energy of about 64-72 kJ/mol), but weakly depend on WF₆ concentrations (of 1/6 order).⁹⁻¹¹

The substrate material was found to have less influence on the formation of film texture at various deposition conditions, such as gas compositions and concentrations and substrate temperatures, as shown by Fig. 2 and 3. Figure 2a and b shows the XRD spectra of tungsten films deposited on nickel and graphite plates, respectively, under the condition (listed in Fig. 2) favoring the formation of the <100> textured films. Figure 2c is the XRD trace for the sample which a <111> textured layer was first grown on the graphite substrate as an intermediate layer and after that, the deposition was carried out under the same condition as that of Fig. 2a and b, but for thickness. The XRD results in Fig. 2 show that these films are all <100> textured with a little difference in orientation degree. In the case of the <111> texture shown in Fig. 3, similar results were observed.

The films deposited on nickel substrates are more textured compared with those deposited on graphite substrates, as shown in Fig. 2a and b and Fig. 3a and b. Such difference is due to the effect of substrate materials and gradually vanishes as films become thicker. A better wettability for tungsten on nickel than on graphite substrates would make nucleation of tungsten crystallites easier, and the film forms a continuous layer with a higher rate and also with smaller crystalline particles. When the crystallites with a specific orientation prefer to grow up, those with other orientations will be gradually terminated in the

Table II. Texture coefficients of CVD tungsten films as a function of H₂ concentrations (samples above the dotted line) and precursor concentrations (samples 1, 5, 7, 12 and those under the dotted line). (Deposition pressure = 200 Torr, total flow = 1700 sccm, Ar gas = balanced, and substrate = graphite.)

Sample no.	Precursors (vol %)		Film deposition temp (°C)	Thickness (μm)	Texture coefficients				
	H ₂	WF ₆			{110}	{200}	{211}	{310}	{222}
1	12	0.6	610	8.6	0.3	0.5	1.2	0.2	2.8
4	47	0.6	610	14	0.0	0.0	— ^a	—	5.0
14	94	0.6	610	3.0	1.0	0.6	1.4	1.0	1.0
15	94	0.6	610	21	—	0.0	—	—	5.0
7	12	0.6	490	9	0.8	0.5	1.4	0.9	1.4
11	47	0.6	490	17	0.2	0.1	0.5	0.1	4.1
16	94	0.6	490	39	0.0	0.1	0.3	—	4.6
2	12	2.4	610	15	0.3	1.1	0.4	3.1	—
5	47	2.4	610	38	0.0	0.0	0.1	—	4.9
17	94	2.4	610	20	0.4	0.1	1.8	0.6	2.1
8	12	2.4	490	9.5	0.2	1.7	0.9	1.6	0.6
12	47	2.4	490	31	0.0	5.0	—	—	—
18	94	2.4	490	15	0.1	3.9	0.1	0.8	0.1
19	94	4.7	610	50	0.1	2.2	0.7	0.2	1.8
20	94	4.7	610	57	0.0	2.8	0.0	0.1	2.1
21	94	4.7	490	26	0.0	4.8	0.0	0.2	—

^a The mark “—” means the corresponding diffraction peak was not found in the spectrum, while the peak with calculated value of 0.0 is of very small relative intensity.

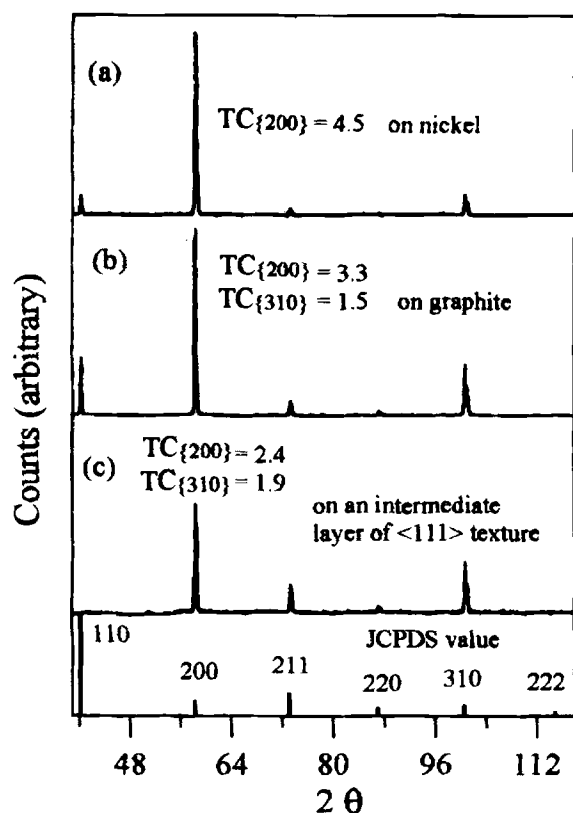


Fig. 2. The X-ray diffraction spectra of CVD tungsten films deposited on (a) nickel plate, (b) graphite plate, and (c) intermediate layer of $\langle 111 \rangle$ texture at the conditions for growing the $\langle 100 \rangle$ textured film. Thickness of film is (a) $6 \mu\text{m}$, (b) $5.7 \mu\text{m}$, and (c) 8 and $6 \mu\text{m}$ for the top film and intermediate layer, respectively. Other parameters are: $\text{WF}_6 = 4.7 \text{ vol } \%$, $\text{H}_2 = 47 \text{ vol } \%$, Ar = balanced, total flow = 1700 sccm , pressure = 200 Torr , and temperature = 490°C .

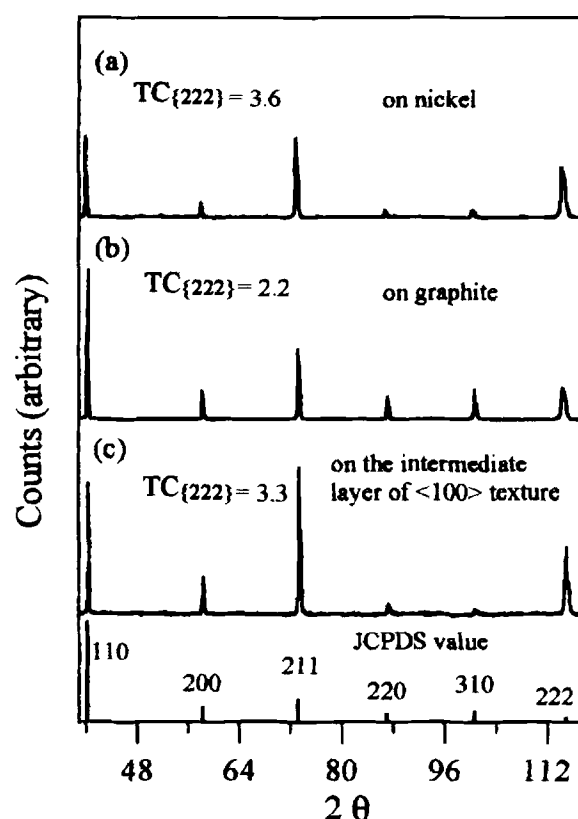


Fig. 3. The X-ray diffraction spectra of CVD tungsten films deposited on (a) nickel plate, (b) graphite plate, and (c) intermediate layer of $\langle 100 \rangle$ texture at the conditions for growing the $\langle 111 \rangle$ textured film. Thickness of film is (a) $8 \mu\text{m}$; (b) $8 \mu\text{m}$; and (c) 6 and $9 \mu\text{m}$, for the top film and intermediate layer, respectively. Other parameters are: $\text{WF}_6 = 0.6 \text{ vol } \%$, $\text{H}_2 = 94 \text{ vol } \%$, Ar = balanced, total flow = 1700 sccm , pressure = 200 Torr , and temperature = 490°C .

subsequent growth. A highly textured film then will form in early growth stage. In addition, a rough surface of graphite substrate also makes the first continuous layer form with more random orientations as well as in later growth stage, as illustrated by Table III showing that deposited on a smoother surface of substrate, the textured film is of higher degree. Thus, with the same film thickness, films deposited on nickel substrates have stronger texture than those deposited on graphite substrates. This difference in the degree of the texture diminishes gradually with the increase of the film thickness.

Crystallographic texture is also a function of film thickness. As shown by samples 10 and 11 in Table I and samples 14 and 15 in Table II, the film was nearly randomly oriented for small thickness value, but strongly textured for large thickness value. Figure 4a-c shows clearly the texture evolution with film thickness: for an as-deposited $\langle 100 \rangle$ textured film with $30 \mu\text{m}$ thickness on graphite, only

$\{200\}$ peak appears in the X-ray diffraction spectrum as shown in Fig. 4a; after being thinned step by step, the relative intensity of $\{200\}$ peak decreases gradually but still dominates Fig. 4b and c. Further thinned to a thickness of $5 \mu\text{m}$, $\{222\}$ and $\{211\}$ peaks are the two with large TC values instead. For the nickel substrate, the similar thickness dependence was observed, but the $\text{TC}_{\{200\}}$ value is always the largest one, when the film was thinned from 30 to $6 \mu\text{m}$ thick. Another example is shown in Fig. 5 (with the same condition as that of sample 16 but for thickness and substrate), in which initially the film on the n-type Si(111) substrate was more randomly textured, but the $\langle 111 \rangle$ texture was nicely developed in the thickness of about $1.1 \mu\text{m}$. This indicates that the texture is formed during the later growth of the film, not at the beginning of the deposition. The formation of crystallographic texture can be understood based on the evolutionary selection theory proposed by Drift,¹² who described that the film growth begins with

Table III. Texture coefficients of tungsten films on nickel plates with different surface preparation. (Plates were polished by $1 \mu\text{m}$ alumina powder and ground by abrasive paper (no. 600), respectively, to create different roughness of plate surface.)

Deposition conditions				Film thickness (μm)	Texture coefficients				
WF_6 (vol %)	H_2	Temp ($^\circ\text{C}$)	Surface preparation		{110}	{200}	{211}	{310}	{222}
0.6	12	490	Polished	10	0.0	0.1	0.0	— ^a	4.9
			Ground	9.5	0.2	0.1	0.7	0.1	3.9
0.6	12	610	Polished	3.6	0.0	0.0	0.0	—	5.0
			Ground	8.6	0.0	0.2	0.3	—	4.5

^a The mark "—" means the corresponding diffraction peak was not found in the spectrum, while the peak with calculated value of 0.0 is of very small relative intensity.

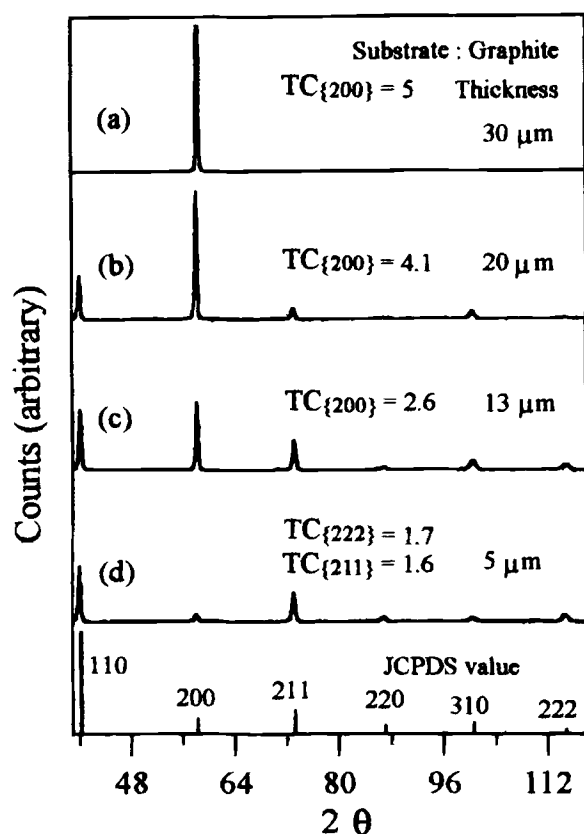


Fig. 4. The X-ray diffraction spectra for the tungsten film after being thinned step by step. Other parameters are: $WF_6 = 2.4$ vol %, $H_2 = 47$ vol %, Ar = balanced, total flow = 1700 sccm, pressure = 200 Torr, temperature = 490°C, and substrate = graphite.

randomly oriented crystallites. Once the crystallites impinge on each other, the growth competition starts between the neighbor crystallites; those crystals with a certain orientation grow faster and get larger at the expense of those with other orientations, and finally the film texture is developed. In this study, the tungsten crystallites are randomly oriented in about several microns thick films on graphite substrates, and about 3000 Å thick films on Si wafers. The growth of the crystal grains with {100} and {111} lattice plane parallel with the surface of substrate are more facilitated than those with other orientations when films were deposited at high and low WF_6 concentrations, respectively. So the <100> and <111> oriented grains grow faster, gradually burying the neighbor grains with different orientations, until, finally, the <100> and <111> orientation become the preferred orientation in films.

Conclusion

CVD tungsten films using H_2 - WF_6 -Ar chemistry have various crystallographic textures, such as the <310>, <100>, and <111>, which depend on the process parameters, especially on WF_6 concentrations and deposition temperatures. A <100> textured film was formed as deposited with high WF_6 concentrations, while a <111> textured film was obtained at low WF_6 concentrations. A higher WF_6 concentration is required for the <100> texture to dominate ($WF_6 \geq 2.4$ vol % for 490°C, while 4.7 for 610°C) as substrate temperature increases. The <111> texture, which was frequently observed in films deposited with high deposition temperatures and gas mixture of high ratios of H_2 to WF_6 , can form at low temperatures (370°C) when the WF_6 concentration used is low enough (0.6 vol %). The <310> texture was observed for films deposited with a narrow range of conditions: low H_2 concentrations (12 vol %) and ratios of H_2/WF_6 (close to 5 or less) and high deposition temperatures (610°C). Different to the previously reported, the H_2 concentrations were observed to be insensitive to the formation of the film texture over a wide range of temperatures (370–610°C) and gas

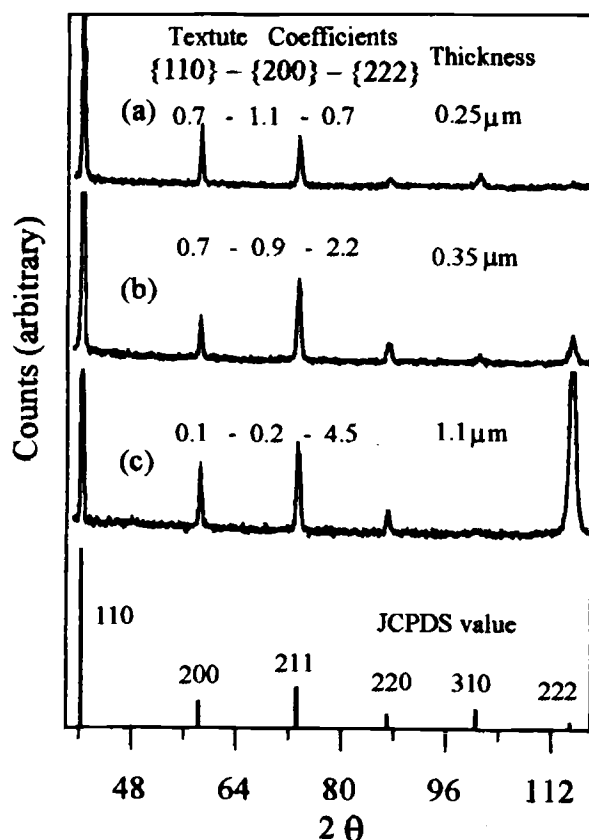


Fig. 5. The X-ray diffraction spectra for the tungsten films of various thickness deposited on n-type Si(111) wafers. The deposition parameters are the same as those of Fig. 3 but for the film thickness and substrate material.

composition (WF_6 : 0.6–4.7 vol %, H_2 : 12–94 vol %) except the narrow region where the <310> texture was formed. The factors dictating the film texture were also observed not to be the same as those dictating the growth rate which strongly depends on H_2 concentrations and deposition temperatures, but weakly depends on WF_6 concentrations. The substrate materials had minimal effect on the formation of the textures of thick films. It has also been shown that the film is randomly textured in the initial stage of growth, then the preferential orientation develops with increasing thickness through the competitive crystal growth.

Acknowledgment

This study was partially supported by National Science Council (NSC 84-2216-E006-012), Taiwan, and is gratefully acknowledged.

Manuscript submitted October 17, 1997; revised manuscript received June 5, 1998.

National Cheng Kung University assisted in meeting the publication costs of this article.

REFERENCES

1. N. D. McMurray, R. H. Singleton, K. E. Muszar, Jr., and D. R. Zimmerman, *J. Met.*, **17**, 600 (1965).
2. M. Schroff and CSF Thomson, in *Proceedings of the Third International Conference on Chemical Vapor Deposition*, F. A. Glaski, Editor, p. 69, American Nuclear Society, Hinsdale, IL (1972).
3. M. S. Haque, U. V. Patel, H. A. Naseem, and W. D. Brown, *J. Electron. Mater.*, **24**, 761 (1995).
4. R. K. Chuzhko, I. V. Kirillov, Yu. N. Golovanov, and A. P. Zakharov, *J. Cryst. Growth*, **3**, 219 (1968).
5. T. I. Kamins, D. R. Bradbury, T. R. Cass, S. S. Laderman, and G. A. Reid, *J. Electrochem. Soc.*, **133**, 2556 (1986).
6. C. S. Barrett and T. B. Massalski, *Structure of Metals*, p. 204, Pergamon, Oxford (1980).
7. Powder Diffraction File, no 4-808, published by the

International Center for Diffraction Data, Swarthmore, PA (1987).

8. J. M. Blocher, Jr., *J. Vac. Sci. Technol.*, **11**, 680 (1974).

9. T. G. M. Oosterlaken, G. J. Leusink, G. C. A. M. Jassen, and S. Radelaar, *J. Electrochem. Soc.*, **143**, 1668

(1996).

10. C. M. McConica and K. Krishnamani, *J. Electrochem. Soc.*, **133**, 2542 (1986).

11. W. A. Bryant, *J. Electrochem. Soc.*, **125**, 1534 (1978).

12. A. van der Drift, *Philips Res. Rep.*, **22**, 267 (1967).

Limitation of HF-Based Chemistry for Deep-Submicron Contact Hole Cleaning on Silicides

M. R. Baklanov,^a E. Kondoh, R. A. Donaton, S. Vanhaelemeersch, and K. Maex

IMEC, B-3001 Leuven, Belgium

ABSTRACT

The limitation of the use of HF-based chemistry for the cleaning of submicron high aspect ratio features is discussed. In this paper we describe the post-dry-etch cleaning of contact holes on TiSi₂. This cleaning process is a combination of the use of oxidizing agents to remove residues consisting of fluorinated polymers and titanium fluorides, and HF-last cleaning to remove SiO₂ on TiSi₂. The HF-last cleaning is necessary to reduce the contact resistance. Two issues are pointed out: a very narrow process window for the HF etch time, and a strong hole size dependence of the contact resistance. These issues are not seen when soft sputter etching is used instead of HF-last cleaning. Concerning the narrow process window, the contact resistance decreases with increasing HF treatment time but increases again after passing through a minimum value. The kinetic study of TiSi₂ etching shows that a preferential etching of the C49 phase takes place during an HF treatment. As a result, the TiSi₂ surface becomes porous, which is thought to decrease the contact area. The hole size dependence is discussed in view of transport of chemical species in the contact hole. It is shown that the size dependence can be explained by assuming an abnormally small diffusion coefficient. HF-SiO₂ chemistry at the sidewall surface of narrow hydrophilic features can explain this abnormally small diffusivity.

Introduction

During the dry etching of Ti or Co silicides in carbon-fluoride plasmas, a complex film containing both metal fluorides and fluorinated polymers (named CF_x polymer hereafter) piles up on the silicide surface. The metal fluorides form on top of the metal silicides as a reaction product of the silicide with fluorine. The CF_x polymer is present mainly in the upper part of the film due to the polymerization reactions of CF_x radicals in plasma.¹⁻³

This complex protective film is crucial in contact hole etching on top of metal silicides. This film practically does not form during etching of SiO₂ but starts to grow up after opening of the silicide surface. Therefore, the presence of this film defines the etch selectivity of SiO₂ toward silicide and can affect important characteristics, such as etch selectivity.¹⁻⁴ The composition, thickness, and protective properties of the film depend on the plasma etch conditions.² The protective film must be fully removed before contact metal plug formation in order to obtain low contact resistance between contact metal plug and silicide.

A traditional and effective way to remove CF_x polymer is etching (ashing) in an oxygen plasma. However, oxygen plasma cannot remove Ti or Co fluorides or oxides because they are not volatile. For instance, TiF₃ and all possible cobalt fluorides have boiling temperatures higher than 1000°C. The sublimation temperature of TiF₄ is acceptably low (284°C), but this compound forms only during the etching when superfluous fluorine is present.³ Therefore, the cleaning of the silicide surface after the contact hole etching should include the combination of both an oxygen plasma for polymer removal and a wet solution for removal of the metal fluorides. It has been established that an effective wet solution for metal fluoride removal is a mixture of sulfuric acid and hydrogen peroxide 4:1 (SPM). This etchant does not attack metal silicide and SiO₂, while it effectively dissolves metal fluorides and removes organic residues.^{2,5} However, after oxygen plasma and SPM treatments, the silicide surface is covered by a thin silicon dioxide film (3–5 nm). This film is presumed to form dur-

ing oxygen plasma and/or SPM treatments, since a native oxide has a smaller thickness. In order to provide a good contact resistance between metal plug and silicide, this SiO₂ film must also be removed. HF-based etchants are extensively used for removal of oxide films from silicon surfaces. However, in the case of silicides, there have been no systematic studies on the removal of surface SiO₂.

The goal of the present work is to study the chemistry of final cleaning of the titanium silicide surface in HF solutions. We mainly focus on HF-last cleaning of contact holes, which are opened in a SiO₂-based interlayer dielectric (ILD) and have TiSi₂ at the bottom. This cleaning process is conducted after the oxygen plasma and SPM treatments. First, the oxygen plasma and SPM treatments are briefly discussed. Next, the effect of the surface SiO₂ film on contact resistance is described. As expected, the contact resistance decreases with HF cleaning time and increases again after having a minimum. In addition, we observe a strong hole size dependence. We then discuss three different mechanisms that explain these behaviors. Etching of SiO₂ is basically responsible for the initial contact resistance reduction. Further etching leads to increase of the contact resistance which originates from surface roughening due to coexistence of C49 and C54 phases. Finally, we discuss the transport of reagents inside the contact holes, which limits the rate of removal of SiO₂ on TiSi₂. The last issue is a specific problem inside narrow and hydrophilic features. We explain the contact hole size dependence of both contact resistance either for via or contact holes, and finally, we compare the results from HF cleaning experiments with the cleaning by low-energy ion sputtering (soft-sputtering etching, SSE).

Experimental

TiSi₂ films were formed on n-type Si(100) wafers. The wafers were cleaned by a standard RCA cleaning. Right before Ti deposition, the wafers were treated by an HF solution in order to produce a hydrogen-passivated surface. Titanium layers were deposited using a magnetron sputtering system. A two-step silicidation was carried out in a rapid thermal processor (RTP) in a nitrogen ambient. Between the two annealing steps, a selective etching in an

^a On leave from Institute of Semiconductor Physics, SB RAS, Novosibirsk 630090, Russia.